ACS Sustainable Chemistry & Engineering

Research Article

pubs.acs.org/journal/ascecg

In Situ Photochemical Synthesis of Zn-Doped Cu_2O Hollow Microcubes for High Efficient Photocatalytic H_2 Production

Longzhou Zhang,[†] Dengwei Jing,[†,‡] Liejin Guo,*[,†] and Xiangdong Yao*[,‡]

[†]International Research Center for Renewable Energy, State Key Laboratory of Multiphase Flow in Power Engineering, Xi'an Jiaotong University, Xi'an 710049, China

[‡]Queensland Micro- and Nanotechnology Centre (QMNC), Griffith University, Nathan, Brisbane, QLD 4111, Australia

Supporting Information

ABSTRACT: Traditionally, Cu ion-based oxide materials are considered not functional as photocatalysts owing to their instability in the photoelectrochemical processes. Here, we report on the light-induced photochemical synthesis of Cu_2O microcubes utilizing $CuWO_4$ as the precursor. It was found that under light irradiation and in the presence of glucose $CuWO_4$ could be reduced *in situ* into Cu_2O with its morphology reassembled from irregular bulk particles to hollow microcubes. Similar morphology transformation could not be observed when CuO or $Cu(NO_3)_2$ were used as precursors. More importantly, the *in situ* photochemical-synthesized Cu_2O naoncubes showed both high activity and excellent stability for glucose reforming under visible light, which overcame the general barrier of Cu_2O instability in photochemical processes. The activity could be remarkably enhanced when 0.1 wt % Zn was doped into the Cu_2O. The excellent performances of the material were related to the existence of hollow microcubes and the modified band structure due to Zn doping.

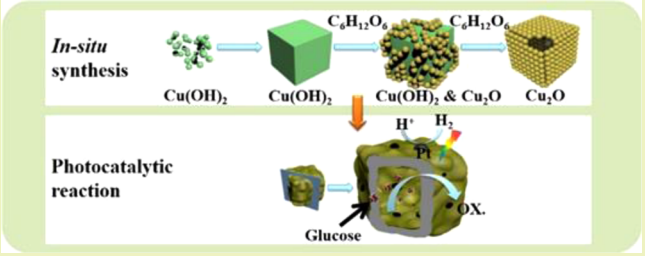

KEYWORDS: *In situ synthesis, Hollow microcubes, Cu_2O, Photocatalysis, H_2 evolution*

INTRODUCTION

Photocatalytic hydrogen production under solar light has been considered as one of the most promising routes for renewable energy conversion.[1−3] It is well accepted that the key to this promising technology is the development of suitable photocatalysts. In view of practical applications, high activity with visible light response, good durability with low toxicity, and low cost are the general requirements for the design of photocatalysts. A large number of photocatalysts have been developed since the first report of this technology by Fujishima and Honda.[4] Binary, ternary, and even more complicated metal oxides and sulfides have been studied. However, few of them simultaneously meet all the requirements mentioned above.[5] We thus pay our attention back to the traditional semiconductors having been considered not suitable as photocatalysts owing to their various inherent drawbacks.

Cuprous oxide, Cu_2O, is an attractive p-type oxide semiconductor with a direct bandgap of 2 eV and a theoretical light-to-hydrogen conversion efficiency of 18%.[6] p-type Cu_2O has a conduction band edge of about −1.35 V vs Ag/AgCl at pH 7, which is sufficiently more negative than the reduction potential of water (about −0.61 V vs Ag/AgCl at pH 7). This means a large overpotential available for hydrogen production. The valence band edge of Cu_2O is at about +0.65 V vs Ag/AgCl at pH 7, also more positive than the oxidation potential of water (about +0.62 V vs Ag/AgCl at pH 7). According to the energy levels, photocatalytic water splitting over Cu_2O under visible light is principally feasible.[7,8] However, the direct evidence showing H_2 evolution from illuminated p-type Cu_2O has been far less than theoretically expected.[8−10] The reason could be the inherent instability of Cu^{1+} ions in the photoelectrochemical processes. For instance, the oxidation of Cu_2O itself to CuO is thermodynamically more favorable than water oxidation. On the contrary, CuO could also be reduced to Cu_2O and finally metallic Cu under photochemical reaction conditions.[11]

To make Cu_2O a stable photocatalyst, the hydrogen production reaction should be kinetically more favorable than other competing side reactions possibly leading to Cu_2O decomposition. Our strategy is to synthesize Cu_2O from a photochemical reaction environment that is similar to the photocatalytic reaction conditions in which Cu_2O is used as a photocatalyst. It is assumed that the Cu_2O obtained in such a strong redox photochemical reaction environment has the inherent advantage to withstand photocorrosion in a kinetically more favorable way. Moreover, modification of the band structure of Cu_2O by appropriate metal ion doping is supposed to make it thermodynamically more favorable for hydrogen production.

To this end, we have chosen glucose both as the precursor material for Cu_2O photochemical synthesis and the sacrificial reagent for photocatalytic hydrogen production. Here, glucose,

Received: January 20, 2014
Revised: April 12, 2014
Published: April 21, 2014

   dx.doi.org/10.1021/sc500045e | ACS Sustainable Chem. Eng. 2014, 2, 1446−1452

as a model compound of the biomass most versatile on earth, was employed as the electron donor for water reduction ensuring that the whole energy conversion process was completely renewable. The feasibility of photocatalytic hydrogen production from glucose has been demonstrated as early as 1980 by Kawai et al. and has undergone tremendous growth.[12,13] For instance,Yu et al. reported on Pt/TiO_2 nanosheets with exposed (001) facets and found high photocatalytic hydrogen generation activity under UV−vis light reaching 134 μmol/h.[14] Up to now, most of the studies have been conducted under UV light, which accounts for only about 4% of the solar spectrum. From the viewpoint of thermodynamics, oxide photocatalysts would be more favorable than sulfides and nitrides.[15] Unfortunately, many oxide semiconductors either have wide band gaps or low conduction band positions that greatly restricted their availability as a visible light-responsive photocatalyst.[16] In previous work, we reported a $Bi_{0.5}Y_{0.5}VO_4$ photocatalyst with a high activity of 10 μmol/h under the irradiation of visible light.[17] To the best of our knowledge, the highest activity of hydrogen generation in the process of glucose reforming under the irradiation of visible light was performed by Li and his co-workers, which was as high as 36 μmol/h, utilizing $Cd_{0.5}Zn_{0.5}S$ as the photocatalyst, showing significant progress forward.[18]

Not long before, we reported a kind of shape-controlled Cu_2O. Through artifical control of its exposure plates, we realized charge separation on the surface of Cu_2O favorable for improving its visible light response. But unfortunately, the activity of Cu_2O was still low in the process of hydrogen generation of glucose reforming, which is only 1.88 μmol/h.[19] In this report, Zn-doped Cu_2O with hollow microcube morphology was prepared by a facile *in situ* photochemical method in the presence of glucose. Steady photocatalytic reforming of glucose under visible light over the as-synthesized Cu_2O photocatalyst was realized. A very low amount of Zn doping, i.e., 0.1 wt %, was found to remarkably enhance the activity of the Cu_2O hollow microcubes. The effects of the Zn doping on the photochemical photophysical properties, crystal structure, and photocatalytic performances were then discussed in detail.

EXPERIMENTAL SECTION

Synthesis of $CuWO_4$ and Zn-Doped $CuWO_4$ Precursors. All chemicals were of analytical grade and used without further purification. Typically, certain amount of $Cu(NO_3)_2{\cdot}6H_2O$ were dissolved in deionized water and precipitated by slow addition of aqueous solution of Na_2WO_4 under continuous stirring. The precipitate was washed with deionized water and dried in an oven at 75 °C for 5 h. The collected product was then calcined at 500 °C for 5 h to obtain $CuWO_4$ as precursor. Various amounts of $Zn(NO_3)_2{\cdot}6H_2O$ was added into the initial solution for the preparation of Zn doped $CuWO_4$.

***In Situ* Photochemical Preparation of Cu_2O and Zn-Doped Cu_2O.** The $CuWO_4$ or Zn-doped $CuWO_4$ precursors were then dispersed in a side irradiated photoreactor containing an aqueous solution of glucose (0.05 mol/L) and NaOH (0.1 mol/L). The photochemical reactor was irradiated by a 300W Xe lamp from 1 to 20 h. The precipitate was then repeatedly washed with deionized water and dried in an oven at 60°C for 10 h to obtain the final Cu_2O and Zn-doped Cu_2O product. The as-prepared samples were denoted as CZO*n* where n is the molar percent of Zn in Cu_2O. It is further denoted as CZO*n*-h, depending on the photochemical reaction time "h" ranging between 3 and 20 h. For comparison, Cu_2O was also prepared by a similar method with commercial CuO and $Cu(NO_3)_2$ as precursors, respectively, by a photochemical reaction of 20 h irradiation.

Material Characterization. The X-ray diffraction (XRD) patterns of catalysts were recorded on Panalytic X'pert Pro X-ray diffractometer equipped with Cu Kα irradiation. All the samples were scanned with a step size of 0.033° 2θ. Diffuse reflectance UV−vis spectra were measured on a Hitachi U-4100 spectrometer, equipped with a labsphere diffuse reflectance accessory. The crystallite morphologic micrograph was determined on a field emission scanning electron microscopy (SEM) JSM-7800F (Japan) and a transmission electron microscope (TEM) FEI Tecnai G2 F30 S-Twin. The X-ray photoelectron spectroscopy (XPS) measurements were conducted on a PHI-550 multifunctional spectrometer. Photoluminescence (PL) spectra were recorded on a Hitachi F-3010 fluorescence spectrophotometer with an integrated time of 0.1 s/nm. Infrared spectroscopy (IR) was measured by time-resolved spectroscopy using a FT-IR spectrometer of the VERTEX series S510. The elemental analysis was completed on a Bruker S4 PIONEER X-ray fluorescence spectrum (XRF), using a Rh target and 4 KW power.

Evaluation of Photocatalytic Activity. For photocatalytic hydrogen evolution, 0.01 g of photocatalyst powder was dispersed by a magnetic stirrer in a side irradiated photocatalytic reactor containing an aqueous solution of glucose (0.05 mol/L) and NaOH (0.1 mol/L). The reaction cell was connected to a gas circulation system, and the hydrogen evolved was analyzed by an online TCD gas chromatograph (NaX zeolite column, argon as carrier gas). The photocatalysts were irradiated with visible light from a 300W Xe lamp, and the UV part of the light was removed by a cutoff filter (λ > 420 nm). Apparent quantum yields were measured and calculated as described in our previous report, using a 420 nm band-pass filter and an irradiatometer.[19] In the experiment, the irradiation power after the band-pass filter was determined to be 0.792 mW/cm^2. The gas product was automatically sampled and analyzed by GC every 10 min during photocatalytic reaction. Before the photocatalytic reaction, the reactor was alternatively evacuated by a vacuum pump and flushed by argon for several times to ensure complete removal of oxygen. As a co-catalyst prompting proton reduction, 0.5 wt % Pt was *in situ* photodeposited on the evaluated photocatalyst from $HPtCl_4$.

RESULTS

Crystalline Structures for Zn-Doped $CuWO_4$ precursors and Cu_2O. Figure 1 shows the X-ray diffraction (XRD) patterns of Zn-doped $CuWO_4$ precursors and various CZO*n* samples. As shown in Figure 1a, all the peaks in the diffraction patterns can be ascribed to the triclinic structure of $CuWO_4$.[20] It was also noticed that diffraction peaks for Zn-doped $CuWO_4$ shifted to lower degrees compared with the pure $CuWO_4$. As shown by the magnified region around 2θ of 15°, even a small amount of Zn doping, i.e., 0.1 wt %, led to a significant shift of XRD peaks. The successive shift of diffraction peaks is attributed to the larger ionic radius of Zn^{2+} than Cu^{2+} ion. XRD patterns for the samples after *in situ* photochemical preparation from this $CuWO_4$ precursor were then recorded. As shown in Figure 1b, all the diffraction peaks can be indexed to the standard cubic phase Cu_2O (JCPDS file no. 05-0667),[21,22] with no other crystalline phase observed. The fact that no diffraction peaks ascribed to $CuWO_4$ could be found in the XRD patterns of the final Cu_2O products proved that all the $CuWO_4$ precursors, regardless of Zn doping, have transformed into Cu_2O. Moreover, no diffractions attributed to ZnO could be found even for 5 wt % Zn doping, indicating successful doping of Zn ions into the matrix of Cu_2O.

It is noteworthy from Figure 1b that the (111) diffraction at 2θ of about 43° for CZO0.1−20 obviously shifts to a lower degree compared to the other samples. However, for Zn doping of more than 0.1%, the (111) diffraction shifts to higher angle

dx.doi.org/10.1021/sc500045e | ACS Sustainable Chem. Eng. 2014, 2, 1446−1452

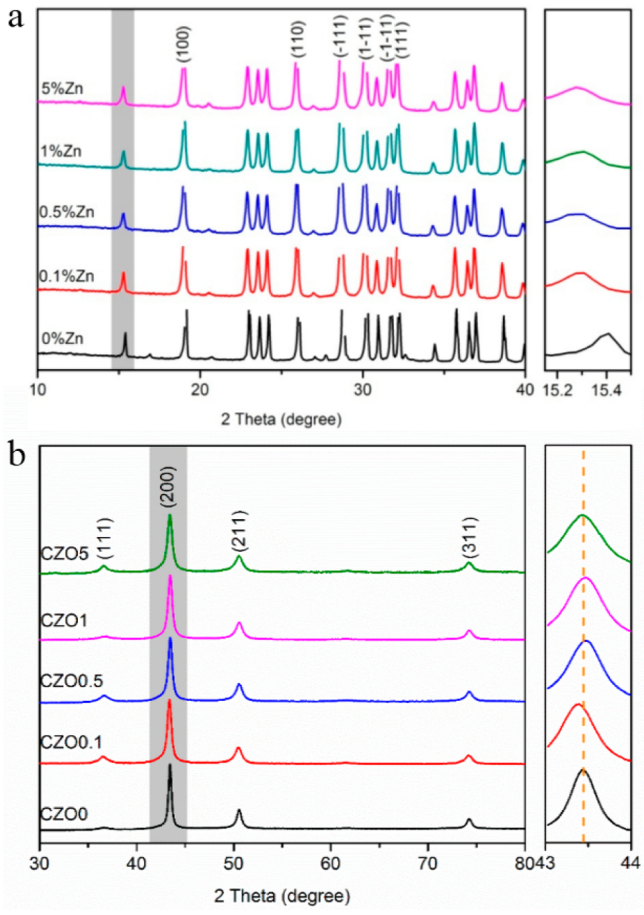

Figure 1. XRD patterns of Zn-doped $CuWO_4$ precursor (a) and various CZO samples reacted for 20 h (b).

again. We have repeatedly prepared Zn-doped Cu_2O samples and obtained similar XRD results. This indicated that the unusual diffraction shift for CZO0.1−20 is not due to experimental errors. At this stage, it can be concluded that a small amount of Zn doping could exert significant effects on the crystal structure of Cu_2O. It is known that Zn^{2+} has a similar ionic radius of 60 Å with Cu^{+} when the coordination number is 4, and cell distortion due to heteroatom substitution is therefore impossible. However, one Zn^{2+} ion should substitute for two Cu^{+} for charge balance if a Zn ion could be successfully doped into Cu_2O. We believe that the unusual diffraction shift for CZO0.1−20 is due, at least in part, to the different valence states between Zn^{2+} and Cu^{1+}. The band gap of CZO0 to CZO5 were calculated as 1.97, 1.89, 1.82, 1.77, and 1.67 eV respectively, according to the Kubelka−Munk function (Figure S4, Supporting Information). Zn doping changed the band gap of Cu_2O undoubtedly. However, the relationship between Zn doping and the modification of the Cu_2O crystal structure needs further investigation.

Morphology Evolution for the Zn-Doped Cu_2O Hollow Microcubes. Morphology evolution for Zn-doped Cu_2O (with CZO0.1−20 as a representative material) was investigated by emission scanning electron microscopy (SEM). As shown in Figure 2a, the $CuWO_4$ precursor is the bundle of aggregates of irregular particles. As a contrast, CZO0.1−20 in Figure 2f shows well-defined hollow microcubes with diameters of around 400 nm. To understand the growth process of the hollow microcubes, SEM characterization was conducted on the CZO0.1 samples collected at different stages of the photochemical synthesis processes. As shown in Figure 2b, at the reaction time of 1 h, the cubic morphology was already formed. As the reaction proceeded, some smaller particles grew at the surface of microcubes, and in the meantime, the inside of the cube began to dissolve.

As shown in Figure S1 of the Supporting Information, the hollow cubic microstructure could not be formed in the absence of light irradiation or using other precursor like copper oxide, and only irregular bundles of Cu_2O were found when copper oxide and Cu^{2+} were utilized as precursor. It becomes

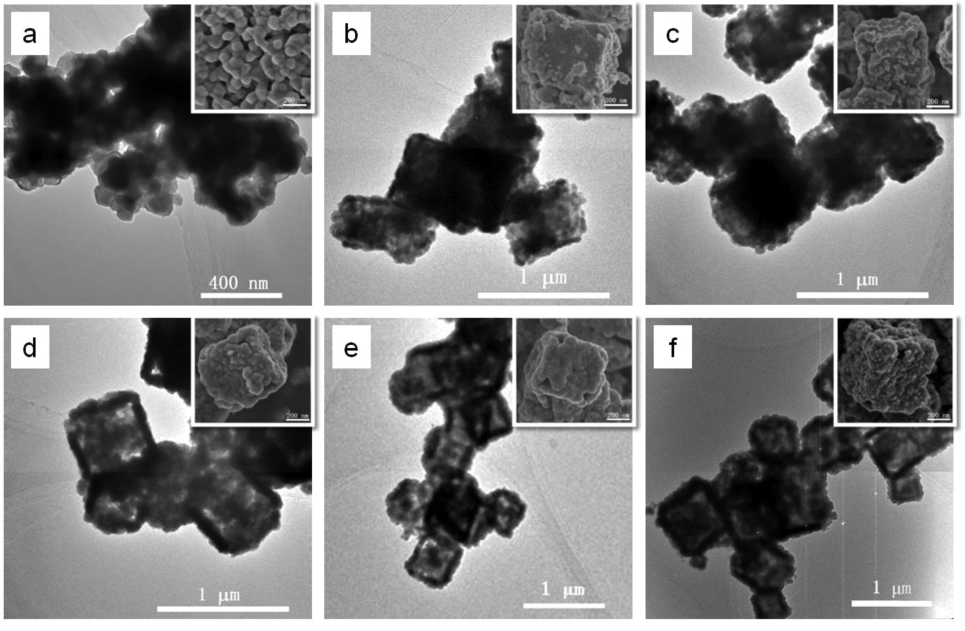

Figure 2. TEM images for CZO0.1 at different stages of the photochemical synthesis process (a) before reaction, (b) 1 h, (c) 2 h, (d) 4 h, (e) 6 h, and (f) 20 h. Corresponding SEM patterns are inset. All scale bars for SEM patterns are 200 nm.

clear that Cu_2O with hollow microcubic morphology can only be prepared with a $CuWO_4$ precursor. It is assumed that due to limited solubility Cu^{2+} in $CuWO_4$ will be gradually released into the reaction solution by dissolution of $CuWO_4$, which in turn results in the gradual reduction and final formation of hollow Cu_2O microcubes.

Photophysical and Photochemical Properties of Various Cu_2O Samples. Figure 3a shows the Fourier transform infrared spectroscopy (FTIR) patterns for the reaction solution taken at various stages of photochemical synthesis of CZO0.1. The C═O peak around 1700 cm^{-1} disappeared after 6 h of reaction. At the same time, a new peak appeared at the wavenumber of about 1600 cm^{-1}, which is the characteristic peak of skeletal vibration of aromatic ring. It is clear that glucose was eventually converted into a kind of aromatic compound after a series of reactions. Although the final state of glucose remains unclear, we believe that the glucose is now in an oxidized state due to the reduction of Cu^{2+}.

Figure 3b shows X-ray photoelectron spectroscopy (XPS) patterns for CZO0.1 samples collected at different stages of the photochemical synthesis. After 1 h of visible light irradiation, the binding energies of Cu 2p3/2 and Cu 2p1/2 peaks were at 932.4 and 952.3 eV, respectively, which are the typical values for Cu^+. Meanwhile, a shakeup line around 945 eV can be observed, which is the paramagnetic chemical state of Cu^{2+} from CuO.[23] It can be concluded that after only 1 h of photoreaction, most of the Cu^{2+} released from $CuWO_4$ has been reduced to Cu^+. Combined with transmission electron microscope (TEM) images in Figure 2, the material at this stage should be solid Cu_2O microcubes containing a small amount of CuO. After 6 h of reaction, the XPS peaks owing to Cu^{2+} become even weaker, indicating almost complete consumption of Cu^{2+} at this stage. The reoxidation of some Cu^+ into Cu^{2+} is considered also inevitable at this stage. The concentration of Cu^{2+} in the reaction solution rapidly decreased with continuous reaction as determined by elemental analysis with XRF (Figure S5, Supporting Information). After 20 h of reaction, all the $Cu^{2+}$was reduced into Cu^+. It is assumed that after a long period of a reduction−reoxidation−reduction process, the Cu^+ in the final Cu_2O should be now in a kinetically stable state that can effectively withstand a strong photocorrosion environment before efficient photocatalytic hydrogen production is achieved.

Fluorescent emission spectra of various CZO samples were further recorded. As shown in Figure 4, a photoluminescence (PL) emission peak at 445 nm and a smaller fluorescent emission peak at 612 nm were noticed for pure Cu_2O (CZO0). The former is considered to be due to the band gap excitation, and the latter is assumed to be from the impurity energy level. With 0.1% Zn doping, the PL emission at 612 nm disappeared, but the peak at 445 nm shows a dramatic increase. Further Zn doping gave rise to a significant decrease in this peak. The PL emission at 445 nm was almost quenched with 5 wt % of Zn doping. The strong PL for CZO0.1−20 indicates that it can be easily excited by light irradiation and produce a large amount of photoexcited charges for subsequent PL emission. It can be concluded at this stage that although the crystalline structure of Cu_2O is not strongly affected by Zn^{2+} doping (Figure 1), the band structure and therefore the photophysical properties of the material could be significantly altered. It seems that an appropriate amount of Zn^{2+} could remarkably improve the lifetime of the photoexcited charges in CZO.

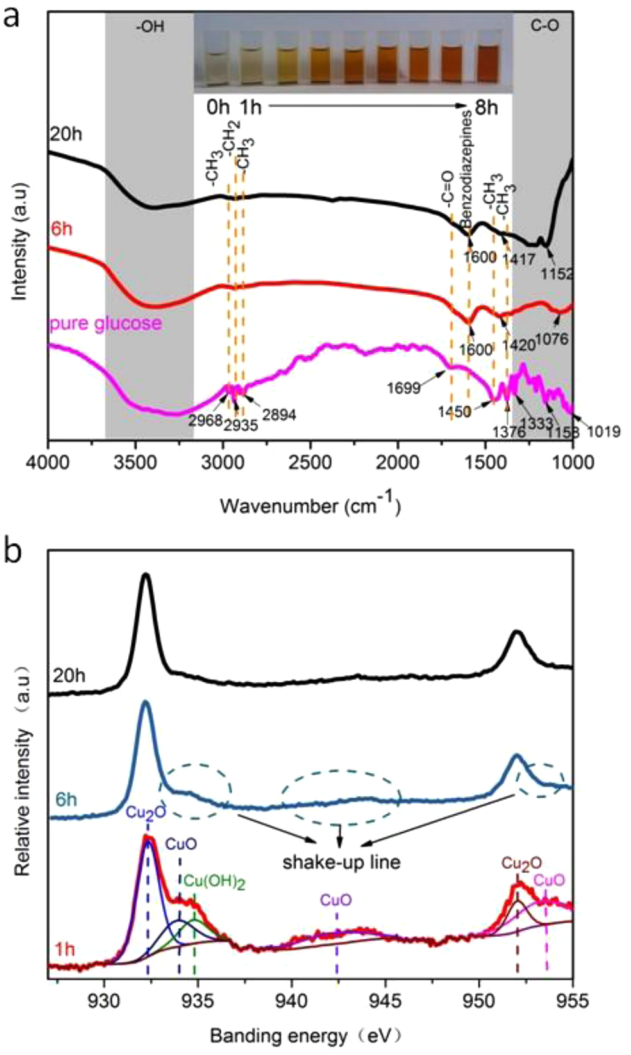

Figure 3. FTIR spectral of reaction solution (a) and XPS pattern of Cu_2O (b) during the photocatalytic synthesis process.

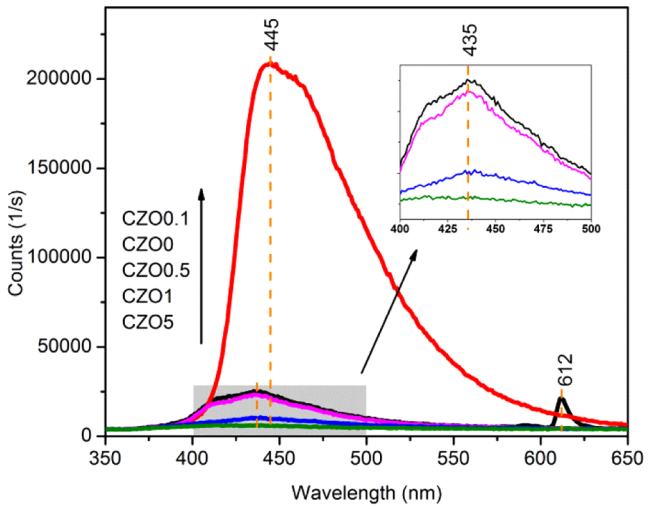

Figure 4. Fluorescent emission spectra of CZO doped with various amount Zn.

dx.doi.org/10.1021/sc500045e | ACS Sustainable Chem. Eng. 2014, 2, 1446−1452

Photocatalytic Reforming of Glucose under Visible Light. The performance of photocatalytic hydrogen production under visible light irradiation for Cu_2O prepared by *in situ* photochemical processing has been evaluated. Samples by two other methods were also evaluated as a comparison. Sample A was synthesized by a hydrothermal method. Samples B and C were synthesized by a photocatalytic method with $CuWO_4$ and commercial CuO as the precursors, respectively. Their corresponding XRD patterns are given in Figure S2 of the Supporting Information. As shown in Figure 5a, Cu_2O synthesized by a photochemical method with $CuWO_4$ as the precursor showed a preferential growth of the (200) crystal plane. Especially, it showed much higher activity for photocatalytic reforming of glucose and also a very good stability compared to the other two samples. As shown in Figure S3 of the Supporting Information, negligible Cu^{2+} could be found for Cu_2O synthesized by the photochemical method with $CuWO_4$ as the precursor after a long photocatalytic reaction. For Cu_2O synthesized with CuO as the precursor, however, a certain amount of Cu^{+} has been oxidized into Cu^{2+}.

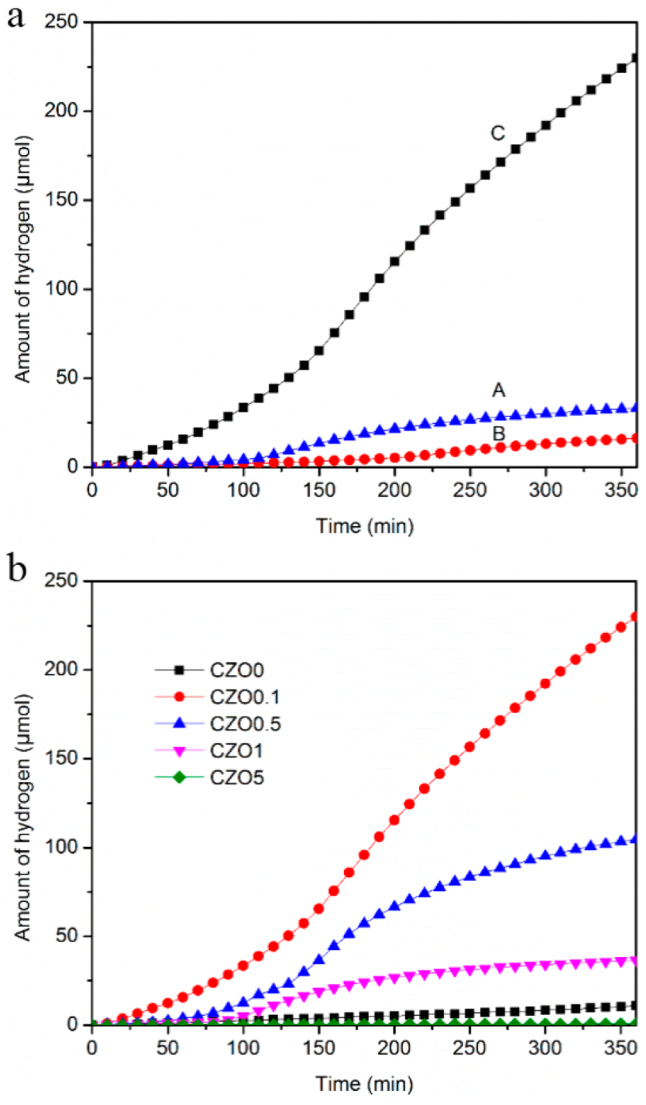

Figure 5. Photocatalytic hydrogen production under visible light irradiation for Cu_2O prepared by various methods. Sample A was synthesized by a hydrothermal method. Samples C and B were synthesized by a photocatalytic method with $CuWO_4$ and commercial CuO as the precursors, respectively. (a) The performance of photocatalytic hydrogen production under visible light irradiation over CZO with different amounts of Zn doping (b).

Photocatalytic activity of CZO with different amounts of Zn doping was then investigated under visible light. As shown in Figure 5b, after 360 min of reaction, total hydrogen production amounts were 10.9, 229, 105, 36.4, and 0.675 μmol, respectively, for CZO with increasing Zn doping in the presence of 0.5 wt % Pt as co-catalyst. Only 10.9 μmol of hydrogen could be observed over the pure Cu_2O sample. The activity showed a dramatic increase in CZO0.1, 21 times that for pure Cu_2O. The apparent quantum yield for hydrogen generation over CZO0.1 at 420 nm was determined to be 38.95%, much higher than our previous report of hydrogen production over $Bi_{0.5}Y_{0.5}VO_4$[20] With a further increase in the Zn-doping amount, however, the hydrogen production drastically dropped. The activity for CZO5 is even lower than for pure Cu_2O. The photocatalytic activity performance is in well agreement with the PL results as shown in Figure 4, indicating that a certain impurity energy level introduced in the Cu_2O energy band will exceedingly increase the lifetime of the excited electrons, which in turn leads to the improvement of hydrogen production activity. It should be also pointed out that the photocatalytic hydrogen production over CZO0.1 is quite stable without showing noticeable deactivation after 360 min of reaction. Recycling hydrogen production experiments were performed. When one round was completed, the gas in the reactor was flushed by argon, and a new round of tests began. From Figure 6, it is shown that CZO0.1 has good stability during the three reaction rounds. The obtained CZO is therefore more favorable than Cu_2O prepared by traditional methods that often show the problem of long-term stability in long-time operations.

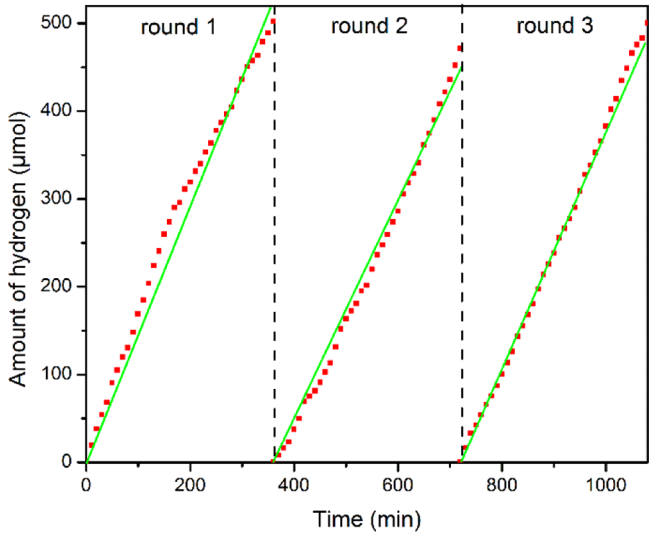

Figure 6. Photocatalytic hydrogen production under visible light irradiation over 60 mg of CZO0.1.

DISCUSSION

So far, Cu_2O with octahedral,[24] cubic,[25] spherical,[26] multi-shelled spherical,[27] and nanocage[28] shapes have been studied. Among the various Cu_2O crystal morphologies, the controlled syntheses of cubic and octahedral structures are perhaps the

dx.doi.org/10.1021/sc500045e | ACS Sustainable Chem. Eng. 2014, 2, 1446−1452

most important. This is because many other structural forms of Cu_2O crystals have been reported to derive from these two basic geometric shapes.[29] There are two major traditional approaches for preparing hollow structures. The most common method involves the use of templates that serve as cores for the subsequent growth of the shells. The cores need to be removed by dissolution, etching, or thermal treatment. Another approach for fabricating hollow structures is the templateless synthesis by self-construction, which is based on the ability of spherical crystallites to stabilize certain crystallographic planes as they undergo two-dimensional (2D) and then 3D aggregation. Obviously our approach represents a completely different approach for Cu_2O synthesis. According to the above discussion, it is speculated that the hollow cubes were formed by the following three steps:

$$CuWO_4 \leftrightarrow Cu^{2+} + WO_4^{2-} \quad \textbf{First step} \tag{1}$$

$$Cu^{2+} + 2NaOH + 2H_2O \rightarrow [Cu(OH)_4]^{2-} + 2Na^+ + 2H^+ \quad \textbf{Second step} \tag{2}$$

$$2[Cu(OH)_4]^{2-} + \text{Glucose} \xrightarrow{h\nu} Cu_2O + \text{Oxidized Glucose} \quad \textbf{Third step} \tag{3}$$

The first step should be slow due to gradual dissolution and release of Cu^{2+} ions from $CuWO_4$. In the second step, Cu^{2+} ion in an aqueous solution first forms $Cu(OH)_2$ and then $[Cu(OH)_4]^{2-}$ in the excessive presence of OH^-. In the third step, due to the strong reducing property of glucose, Cu^{2+} was reduced into Cu_2O. The formation process of the hollow Cu_2O microcubes is schematically illustrated in Figure 7. The

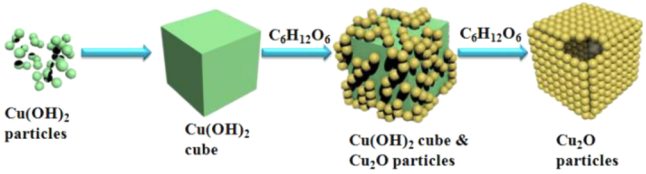

Figure 7. Schematic illustration for the formation of the hollow structures of CZO.

spherical nanocrystallites first undergo 2D and then 3D aggregation to form a microcube. After the surface of the microcube was fully covered with nanoparticles, the microcube dissolved from inside and finally formed a hollow microcube. The hollow microcube morphology is believed to be especially beneficial for photocatalytic reforming of large organic materials such as glucose. In this case, the porous microcube can act as a microreactor for photocatalytic reaction, and the light irradiation can penetrate into the inside of the microreactor due to its porous structure. The obtained hollow microcube is also expected to be available as a microreactor for other extended applications. The principle pattern of the photocatalytic reaction is shown in Figure 8.

In our work, both the Cu_2O and 0.1 wt % Zn-doped Cu_2O showed quite stable activity for hydrogen production. Especially, the latter one showed very high activity for glucose photocatalytic reforming. Traditionally, the instability of Cu^+ ions in photoelectrochemical processes is thermodynamically inevitable. For instance, the oxidation of Cu_2O itself to CuO has a redox potential of −0.05 V, which is more favorable than water oxidation. On the contrary, CuO could be reduced to

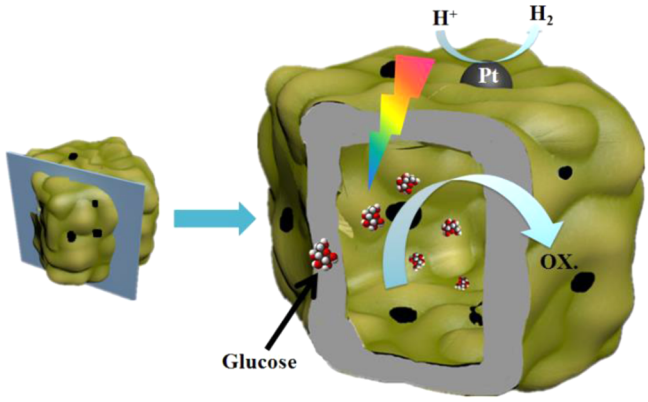

Figure 8. Mechanism for photocatalytic reaction over one single hollow CZO microcube.

Cu_2O and finally metallic Cu under photochemical reaction conditions. During our *in situ* photochemical synthesis of CZO, however, it is believed that a certain amount of Cu^+ could be reoxidized. Due to the existence of excessive glucose, it will be reduced again. As shown by the XPS result in Figure 3b, after 20 h of reaction, only Cu^+ exists. It is supposed that after a long period of a reduction−reoxidation−reduction process, the Cu^+ in the final Cu_2O should be now in a configuration that is kinetically favorable for the strong photocorrosion environment. Comparatively, Cu_2O synthesized by the traditional hydrothermal method was quite instable after 20 h of reaction as is shown in Figure 3s by XPS results, in which the satellite peak of CuO is clearly observed. Therefore, the *in situ*-formed Cu_2O from $CuWO_4$ should be kinetically more favorable for a hydrogen production reaction than other competing side reactions that could possibly lead to Cu_2O decomposition, as shown by eqs 4 and 5.[6]

$$Cu_2O + H_2O + 2e \leftrightarrow 2Cu + 2OH^- \quad E = 0.47\ \text{V vs NHE} \tag{4}$$

$$2CuO + 2H_2O + 4e \leftrightarrow Cu_2O + 4OH^- \quad E = 0.60\ \text{V vsNHE} \tag{5}$$

Here, we reported the *in situ* photocatalytic synthesis of Cu_2O microcubes with $CuWO_4$ as the precursor, considering that traditionally Cu ion-based oxide material was not suitable as a photocatalyst due to the instability of Cu^{2+} ions in photoelectrochemical processes. It was found that under the light irradiation and in the presence of glucose, $CuWO_4$ was reduced *in situ* into Cu_2O with its morphology reassembled from irregular bulk particles to hollow microcubes. The strong photocorrosion environment for the Cu_2O *in situ* crystal growth is believed to be crucial for its stability in the following photocatalytic reaction. It was further found that a small amount of 0.1 wt % Zn doping could remarkably enhance the activity of Cu_2O. Cu_2O with 0.1 wt % Zn doped showed remarkable photocatalytic activity with an apparent quantum yield of 38.95%. Although the rate of hydrogen generation is still lower than that of Pt/TiO_2 nanosheets performed under UV−vis light, it is the highest value reported for photocatalytic hydrogen generation over oxide materials in a glucose system and under visible light. Our finding is believed to be useful for development of Cu^+-based photocatalysts and provides a new synthetic method. The obtained hollow microcubes are also

expected to be available as microreactors for other extended applications.

■ ASSOCIATED CONTENT

Supporting Information

SEM images for Cu_2O prepared by a photocatalytic method with commercial CuO and Cu^{2+} as precursors, XPS pattern of Cu_2O after photocatalytic reaction, and XRD patterns of Cu_2O prepared by various methods. This material is available free of charge via the Internet at http://pubs.acs.org.

■ AUTHOR INFORMATION

Corresponding Authors

*E-mail: lj-guo@mail.xjtu.edu.cn (L.G.).
*E-mail: X.Yao@griffith.edu.au (X.Y.).

Notes

The authors declare no competing financial interest.

■ ACKNOWLEDGMENTS

The authors gratefully acknowledge the financial supports of the Australian Research Council (ARC), National Natural Science Foundation of China (No. 51121092, 21276206), Fundamental Research Funds for the Central Universities, and National 863 Program of China (No. 2012AA051501).

■ REFERENCES

(1) Kudo, A.; Miseki, Y. Heterogeneous photocatalyst materials for water splitting. *Chem. Soc. Rev.* **2009**, *38*, 253−278.
(2) Tachibana, Y.; Vayssieres, L.; Durrant, J. R. Artificial photosynthesis for solar water-splitting. *Nat. Photonics* **2012**, *6*, 511−518.
(3) Li, Z.; Luo, W.; Zhang, M.; Feng, J.; Zou, Z. Photoelectrochemical cells for solar hydrogen production: current state of promising photoelectrodes, methods to improve their properties, and outlook. *Energy Environ. Sci.* **2013**, *6*, 347−370.
(4) Fujishima, A.; Honda, K. Electrochemical photolysis of water at a semiconductor electrode. *Nature* **1972**, *238*, 37−38.
(5) Jing, D.; Yao, S.; Chen, P.; Liu, M.; Shi, J.; Zhao, L.; Yan, W.; Guo, L. A multichannel system for rapid determination of the activity for photocatalytic H_2 production. *AIChE J.* **2012**, *58* (11), 3593−3596.
(6) Paracchino, A.; Laporte, V.; Sivula, K.; Grätzel, M.; Thimsen, E. Highly active oxide photocathode for photoelectrochemical water reduction. *Nat. Mater.* **2011**, *10*, 456−461.
(7) Jongh, P. E.; Vanmaekelbergh, D.; Kelly, J. Cu_2O: A catalyst for the photochemical decomposition of water? *Chem. Commun.* **1999**, *12*, 1069−70.
(8) Nian, J.; Hu, C.; Teng, H. Electrodeposited p-type Cu_2O for H_2 evolution from photoelectrolysis of water under visible light illumination. *Int. J. Hydrogen Energy* **2008**, *33*, 2897−2903.
(9) Hara, M.; Kondo, T.; Komoda, M.; Ikeda, S.; Shinohara, K.; Tanaka, A.; Kondo, J. N.; Domen, K. Cu_2O as a photocatalyst for overall water splitting under visible light irradiation. *Chem. Commun.* **1998**, 357−358.
(10) Hu, C.; Nian, J.; Teng, H. Electrodeposited p-type Cu_2O as photocatalyst for H_2 evolution from water reduction in the presence of WO_3. *Sol. Energy Mater. Sol. Cells* **2008**, *92*, 1071−1076.
(11) Zheng, J.; Song, G.; Kim, C.; Kang, Y. Facile preparation of p-CuO and p-CuO/n-$CuWO_4$ junction thin films and their photoelectrochemical properties. *Electrochim. Acta* **2012**, *69*, 340−344.
(12) Kawai, T.; Sakata, T. Conversion of carbohydrate into hydrogen fuel by a photocatalytic process. *Nature* **1980**, *286*, 474−476.
(13) Kawai, M.; Kawai, T.; Tamaru, K. Production of hydrogen and hydrocarbon from cellulose and water. *Chem. Lett.* **1981**, *8*, 1185.
(14) Yu, J.; Qi, L.; Jaroniec, M. Hydrogen production by photocatalytic water splitting over Pt/TiO_2 nanosheets with exposed (001) facets. *J. Phys. Chem. C* **2010**, *114* (30), 13118−13125.
(15) Maeda, K.; Domen, K. Photocatalytic water splitting: recent progress and future challenges. *Chem. Lett.* **2010**, *1*, 2655−2661.
(16) Shi, J.; Guo, L. ABO_3-based photocatalysts for water splitting. *Prog. Nat. Sci.* **2012**, *22* (6), 592−615.
(17) Jing, D.; Liu, M.; Shi, J.; Tang, W.; Guo, L. Hydrogen production under visible light by photocatalytic reforming of glucose over an oxide solid solution photocatalyst. *Catal. Commun.* **2010**, *12* (4), 264−267.
(18) Li, Y.; Gao, D.; Peng, S.; Lu, G.; Li, S. Photocatalytic hydrogen evolution over Pt/$Cd_{0.5}Zn_{0.5}S$ from saltwater using glucose as electron donor: An investigation of the influence of electrolyte NaCl. *Int. J. Hydrogen Energy* **2011**, *36* (7), 4291−4297.
(19) Zhang, L.; Shi, J.; Liu, M.; Jing, D. Photocatalytic reforming of glucose under visible light over morphology controlled Cu_2O: Efficient charge separation by crystal facet engineering. *Chem. Commun.* **2014**, *50* (2), 192−194.
(20) Pandey, P.; Bhave, N.; Kharat, R. Spray deposition process of polycrystalline thin films of $CuWO_4$ and study on its photovoltaic electrochemical properties. *Mater. Lett.* **2005**, *59*, 3149−3155.
(21) International Center for Diffraction Data. Powder Diffraction Files of the Joint Committee on Powder Diffraction Standards, 2001, Card No. 05-0667.
(22) Son, D.; Oh, D.; Kim, T. Structural and optical properties of Cu_2O nanoparticles formed on Al_2O_3 substrates using spin coating and thermal treatment. *Phys. E* **2010**, *43*, 13−16.
(23) Ghijsen, J.; Tjeng, L.; Elp, J.; Eskes, H.; Westerink, J.; Sawatzky, G.; Czyzyk, M. Electronic structure of Cu_2O and CuO. *Phys. Rev. B* **1988**, *38*, 11322−11330.
(24) Lu, C.; Qi, L.; Yang, J.; Wang, X.; Zhang, D.; Xie, J.; Ma, J. One-pot synthesis of octahedral Cu_2O nanocages via a catalytic solution route. *Adv. Mater.* **2005**, *17*, 2562.
(25) Teo, J.; Chang, Y.; Zeng, H. Fabrications of hollow microcubes of Cu_2O and Cu via reductive self-assembly of CuO nanocrystals. *Langmuir* **2006**, *22*, 7369.
(26) Chang, Y.; Teo, J.; Zeng, H. Formation of colloidal CuO Nanocrystallites and Their Spherical Aggregation and Reductive Transformation to hollow Cu_2O nanospheres. *Langmuir* **2005**, *21*, 1074.
(27) Xu, H.; Wang, W. Template synthesis of multishelled Cu_2O hollow spheres with a single-crystalline shell wall. *Angew. Chem.* **2007**, *46*, 1489.
(28) Kuo, C.; Huang, M. Fabrication of truncated rhombic dodecahedral Cu_2O nanocages and nanoframes by particle aggregation and acidic etching. *J. Am. Chem. Soc.* **2008**, *130*, 12815−12820.
(29) Ho, J.; Huang, M. Synthesis of submicrometer-sized Cu_2O crystals with morphological evolution from cubic to hexapod structures and their comparative photocatalytic activity. *J. Phys. Chem. C* **2009**, *113* (32), 14159−14164.